Journal of Inflammation Research Dovepress

Open Access Full Text Article ORIGINAL RESEARCH

Sodium Propionate Alleviates Atopic Dermatitis by Inhibiting Ferroptosis via Activation of LTBP2/FABP4 Signaling Pathway

Anni Xie[1,*], Weijia Li[2,*], Danni Ye[1], Yue Yin[3], Ran Wang[1], Min Wang[1], Renqiang Yu[1]

[1]Department of Neonatology, Affiliated Women's Hospital of Jiangnan University, Wuxi Maternity and Child Health Care Hospital, Wuxi, 214002, People's Republic of China; [2]Department of Biochemistry and Molecular Biology, Franklin & Marshall College, Lancaster, PA, 17603, USA; [3]Suzhou Medical College, Soochow University, Suzhou, 215123, People's Republic of China

*These authors contributed equally to this work

Correspondence: Min Wang; Renqiang Yu, Department of Neonatology, Affiliated Women's Hospital of Jiangnan University, Wuxi Maternity and Child Health Care Hospital, Wuxi, 214002, People's Republic of China, Tel +86 510 82725161, Fax +86 510 82725094, Email wangmin2072@163.com; yurenqiang@jiangnan.edu.cn

Background: Atopic dermatitis (AD) is a common pediatric skin disease, with recent studies suggesting a role for ferroptosis in its pathogenesis. Sodium propionate (SP) has shown therapeutic potential in AD, yet its mechanism, particularly regarding ferroptosis modulation, remains unclear. This study aims to explore whether SP alleviates AD by modulating ferroptosis-related pathways through bioinformatic and in vitro analyses.

Methods: We analyzed the GEO AD cohort (GSE107361). Ferroptosis-related genes was compiled from the GeneCards Database and SP-associated therapeutic target genes were obtained from Swiss Target Prediction. To explore potential biological mechanisms, we employed Gene Set Variation Analysis (GSVA), Gene Ontology (GO), and Kyoto Encyclopedia of Genes and Genomes (KEGG) analyses. Weighted Gene Co-expression Network Analysis (WGCNA) and differential expression analysis identified key gene modules. We also established TNF-α/IFN-γ induced AD cell models using HaCat cells and collected cell samples for further experiments.

Results: The GSVA analysis demonstrated that ferroptosis-related genes could differentiate between healthy children and those with AD. The identified module includes genes with correlated expression patterns specifically linked to AD. Analysis using three algorithms identified potential therapeutic targets of SP. We screened 51 key genes related to AD and ferroptosis, selecting cyclin-dependent kinase 1 (CDK1) and latent transforming growth factor beta binding protein 2 (LTBP2) as co-expressed genes. Machine learning identified fatty acid binding protein 4 (FABP4) as a significant gene intersection of the 51 key genes. The bioinformatics analysis results were validated through cell experiments, showing that SP treatment increased the expression of the damaged skin genes loricrin (LOR) and filaggrin (FLG).

Conclusion: Our study indicates that SP may alleviate AD symptoms by modulating ferroptosis through the LTBP2/FABP4 pathway.

Keywords: atopic dermatitis, ferroptosis, bioinformatics, propionate

Introduction

Atopic dermatitis (AD) is a chronic inflammatory skin disease with significant variations in prevalence among children, ranging from 2.7% to 20.1% among 65,661 participants.[1] This skin disorder causes itching, one of its most unbearable symptoms. The pathophysiology of AD involves various immune cells and chemokines, including interleukin-4 (IL-4) and interleukin-13 (IL-13).[2] In chronic phase, Th1 polarization and the Th17 pathway are impaired.[3] Cell death has long been a focal point of research on various diseases. Recent studies have demonstrated that AD is closely associated with pyroptosis[4,5] and apoptosis.[6,7] These cell death patterns are significantly linked to oxidative stress.[8,9] Many studies are exploring emerging treatments that show great promise for AD. Ferroptosis, a novel mode of cell death, has been

Received: 4 October 2024
Accepted: 24 November 2024
Published: 29 November 2024

identified in immune diseases.[10,11] Recent studies indicate that immune cells can undergo ferroptosis.[10] Ferroptosis plays a crucial role in regulating oxidative stress and the inflammatory response.[12] Inhibiting ferroptosis can significantly alleviate oxidative stress and reduce disease states, such as cognitive impairment in rats with chronic cerebral hypoperfusion,[13] corneal damage in xerophthalmia[14] and emphysema.[15] Blocking ferroptosis can diminish the inflammatory response.[16,17] Studies have shown that inhibiting ferroptosis alleviates psoriasis-related inflammation,[18] reduces skin inflammation caused by UV-B radiation[19] and diminishes cartilage inflammation in arthritis.[20] Researches show that hydrogels can reduce scratch-induced intercellular inflammation by scavenging intracellular reactive oxygen species (ROS). They alleviate skin inflammation and help reconstruct the skin barrier in AD mice.[21–23] Oxidative stress is associated with inflammation.[24,25] Significant oxidative stress has also been detected in ferroptosis.[10,25] Analyses of public databases have demonstrated that ferroptosis-related genes play significant roles in AD.[26] Ptgs2 is a crucial gene involved in ferroptosis.[27] A recent bioinformatics analysis examined four datasets and identified four ferroptosis-related genes (ALOXE3, FABP4, MAP3K14, and EGR1) as potential therapeutic biomarkers for AD.[26] This study aimed to identify and validate the therapeutic targets of ferroptosis in AD.

Current treatment options for AD are categorized as local and systemic therapies, including corticosteroids, calcineurin inhibitors, and Janus kinases (JAK) inhibitors.[28] Researchers have primarily focused on baricitinib and upadacitinib among the JAK inhibitors. Studies indicate that baricitinib effectively treats moderate to severe AD by significantly improving symptoms and reducing pruritus.[29] Upadacitinib also demonstrates good efficacy and safety; however, predict its effectiveness need to be further investigated.[30–32] These JAK inhibitors possess distinct advantages in the treatment of AD, providing more treatment options and references for clinicians and patients.

Multiple studies prove that probiotic interventions enhance AD outcomes in animals and infants[33–35] and positively influence intestinal flora.[36,37] Propionate, a short-chain fatty acid, is produced by intestinal flora during dietary fiber metabolism. Studies indicate that propionate effectively reduces oxidative stress and inflammatory responses.[38–40] A study utilizing hydrogen peroxide (H_2O_2) to induce oxidative stress in HaCat cells found that cellular damage caused by oxidative stress could be reversed by activation of the Nrf2 signaling pathway.[41] Furthermore, the chemical-induced AD-like inflammation in mice can be mitigated by molybdenum nanoparticles through regulating the ROS-mediated Nrf2 /HO-1 signaling pathway.[42] Our previous study shown that SP protects against LPS-induced inflammation in an Nrf2-dependent manner, exhibiting both antioxidant and anti-inflammatory properties.[43] Another study revealed that the short-chain fatty acid sodium butyrate alleviates autoimmune uveitis through the Nrf2/HO-1 pathway.[44] Studies have shown that propionate can enhance forms of programmed cell death[45] such as pyroptosis,[46] However, its effect on ferroptosis remains unclear. Previous studies indicate that the levels of propionate in AD mice and patients are generally reduced, and the concentration of propionate on the skin surface of AD patients is significantly lower than that of healthy individuals, and the local application of propionate alleviates the skin inflammation in AD mice by inhibiting IL-33.[47] In addition, propionate can directly regulate the production of sensory channels and neuropeptides, inhibiting skin itching.[48] This article explores the ameliorative effects of SP on AD by inhibiting ferroptosis, with the hope that it can contribute to the treatment of AD. This study aimed to investigate the gene signature of pediatric AD and potential treatment options. We downloaded the original data (GSE107361) from the Gene Expression Omnibus and identified DEGs, which were analyzed by using gene ontology (GO) and pathway enrichment analysis.

Materials and Methods

Data Download and Preprocessing

The datasets utilized in this study were obtained from the Gene Expression Omnibus (GEO) database (http://www.ncbi.nlm.nih.gov/geo/),[49] specifically dataset GSE107361. It contains gene expression data from the skin tissue samples of both healthy and ill children. According to Article 32 of the "Guidelines for Ethical Review of Life Science and Medical Research Involving Human Beings" issued in China in 2023, human data or biological samples may be exempt from ethical review if the research does not harm individuals, involve sensitive personal information, or pursue commercial interests. This exemption is intended to reduce the burden on researchers and promote life science and medical research.

Rule (1) specifies that research using publicly available data must be obtained legally or through non-intrusive observation.

Acquisition of Ferroptosis-Related Genes

In this study, a total of 1,407 ferroptosis-related genes were identified using data from the GeneCards database (https://www.genecards.org/).

Acquisition of SP Therapeutic Target-Related Genes

In this study, a total of 24 therapeutic target-related genes associated with SP were obtained from a combination of the Swiss Target Prediction (https://SwissTargetPrediction.ch/).

Identification of Differentially Expressed Genes (DEGs) Analysis

The differential expression of mRNA in the dataset GSE107361 was analyzed using the limma package in R software (version 4.2.2). Genes meeting the criteria of adjusted P-values <0.05 and absolute log2 fold changes (the AD group/the control group) > 1 were classified as DEGs.

Gene Ontology (GO) Annotation Analysis

Gene Ontology (GO) annotation analysis was conducted using the "cluster Profiler" R package in this study. A significance threshold of P-value < 0.05 was established to identify statistically significant results in the analysis.

Kyoto Encyclopedia of Genes and Genomes (KEGG) Annotation Analysis

In this study, Kyoto Encyclopedia of Genes and Genomes (KEGG) Annotation Analysis was conducted using the "cluster Profiler" R package. A statistical significance threshold of P-value < 0.05 was proved to distinguish significant results in the analysis.

Weighted Gene Co-Expression Network Analysis (WGCNA)

As a systematic biological approach, WGCNA was employed to reveal the gene association patterns among different samples and to detect the candidate biomarker genes or therapeutic targets according to the interconnectedness of gene sets together with the association between gene sets and phenotypes. We performed WGCNA on GSE107361 to obtain modules closely related to AD. Following a filtering criterion of 0.5, the first step involved eliminating genes and samples that did not meet the criteria using the goodSamplesGenes function. This was followed by the construction of a scale-free co-expression network. For the purpose of calculating adjacencies, a soft threshold of $\beta = 10$ and a scale-free fit of $R^2 = 0.9$ were utilized. These adjacencies were subsequently converted into a topological overlap matrix (TOM), which was used to assess gene ratios and dissimilarities. Genes with similar expression patterns were grouped into modules through average linkage hierarchical clustering. Preferring larger groupings, the threshold for module size was set at a minimum of 50. The next step involved determining the dissimilarity between the module eigengenes. Finally, the eigengene network was visualized.

Identification of Ferroptosis-Related Diagnostic Biomarkers for AD

The target genes related to ferroptosis were screened in genecards, and the ferroptosis-related genes were compared with the AD target genes.

Identification of SP Therapeutic Target-Related Genes from Swiss Target Prediction

SP therapeutic target-related genes were obtained from Swiss Target Prediction.[50]

Gene Set Enrichment Analysis (GSEA)

To gain deeper insight into the biological processes of ferroptosis-related genes, we performed GSEA[51] as well as ssGSEA of the core genes using the ClusterProfiler software package[52] and the GSEA software package. We considered an adjusted p-value < 0.05 and a false discovery rate (FDR) (q-value) < 0.25 were used as the cut-off criteria.

Machine Learning

We employed three machine learning algorithms: LASSO, Random Forest (RF), and Support Vector Machine with Recursive Feature Elimination (SVM-RFE) to perform a comprehensive screening of candidate genes associated with selected genes.[53–55] To implement the LASSO algorithm, we utilized the glmnet package and employing ten-fold cross-validation to identify significant genes. The RF algorithm was executed using the random Forest package, from which we selected the top 11 genes as potential candidates. For the SVM-RFE algorithm, we leveraged the e1071 package and determined the optimal number of genes based on their accuracy. The resulting gene list comprised key genes, and we applied the three machine learning algorithms separately to identify candidate genes related to ferroptosis in AD. Finally, by intersecting the outcomes obtained from the three distinct machine learning approaches, we derived the candidate genes associated with both ferroptosis and SP therapy.

Protein–Protein Interaction Network Construction

To understand the progression of AD and to explore the interactions among protein-coding genes, we constructed a Protein-Protein Interaction (PPI) network utilizing the STRING database. We examined intersecting genes using the Search Tool for the Retrieval of Interacting Genes (STRING; http://string-db.org) (version 12.0)[56] to analyze the biological relationships that exist between these genes. This interaction network illustrates relationships between proteins, including upstream and downstream regulatory pathways as well as direct binding interactions. Interactions with a composite score exceeding 0.4 were deemed statistically significant. We employed Cytoscape (http://www.cytoscape.org) (version 3.10.2)[57] to visualize this PPI network and to analyze key functional modules using the internal plug-in for molecular complex detection (MCODE). Set the selection criteria were set as follows: K-core = 2, degree cutoff = 2, maximum depth = 100, and node score cutoff = 0.2. KEGG and GO analyses of the involved modular genes were conducted using the clusterProfiler package.

Cell Cultures

Human keratinocytes cells (HaCaT) were obtained from iCell Bioscience Inc. (Shanghai, China) and cultured in Dulbecco's Modified Eagle medium (DMEM) containing 10% fetal bovine serum (FBS), 100 U/mL penicillin, and 100 μg/mL streptomycin at 37°C in 21% oxygen and 5% CO_2. To investigate the anti-AD effect of SP in inhibiting inflammation and promoting skin barrier differentiation, normal HaCaT cells were treated with various concentrations of SP. The effect of the treatment on cell viability was detected by CCK8 assay method. HaCaT cells were treated with 10 μg/L TNF-α/IFN-γ to establish an AD cell model.

HaCaT Cell Line Proliferation and Cytotoxicity

For proliferation assays, HaCaT WT, AD model cells, and intervened cells were seeded at a density of 1,000 cells per well in a standard cell culture 96-well plate. Proliferation was assessed using the CCK-8 proliferation assay kit (Apex Bio) in accordance with the manufacturer's guidelines. Cytotoxicity was measured using the LDH Cytotoxicity kit (Apex Bio) following the manufacturer's instructions.

Western Blot Analysis

The levels of CDK1, FABP4, LTBP2, LOR, FLG, and GAPDH were assessed using Western blotting. Protein concentration was determined by BCA method. Subsequently, the proteins (10 μg) were separated via 10% SDS-PAGE and transferred onto PVDF membranes. The membranes were blocked with 5% skimmed milk powder for 2.5 hours, followed by overnight incubation with primary antibodies (1:1000) at 4°C for 12 hours, and then incubated with secondary antibodies (1:5000) for 1 hour. Band visualization was performed using a Tanon 5200 imager. Each experiment was conducted in triplicate. The CDK1, FABP4, and LOR antibodies were obtained from MedChemExpress (Shanghai, China), the LTBP2 antibody was sourced from Biodragon (Suzhou, China), the FLG antibody was acquired from ABclonal (Wuhan, China), and the GAPDH antibody was obtained from ProteinTech (Wuhan, China).

Quantitative Real-Time Reverse Transcription PCR (qRT-PCR)

In this study, qRT-PCR was employed to assess the mRNA levels of TSLP, FLG, LOR, IL-4, IL-13, CCL17, GPX4, and PTGS2 in HaCaT cells. Trizol was used to extract total RNA from cells. Reverse transcription was performed with the PrimeScript RT Reagent Kits. qRT-PCR was conducted using quantitative PCR with SYBR Premix Ex Taq™ (Vazyme, Nanjing, China) and the LightCycler® 480 detection PCR system (Roche, Foster City, CA, USA). mRNA expression levels were quantified using the comparative cycle threshold (Ct) method, where the relative quantification of target transcript levels was determined by subtracting the Ct values of target genes from the Ct values of GAPDH. The primers used in this study are as follows: TSLP: F, ACCTTCAATCCCACCGCCGGC, R, GGCAGCCTTAGTTTTCATGGCGA; FLG: F, AAAGAGCTGAAGGAACTTCTGG, R, AACCATATCTGGGTCATCTGG; LOR: F, GCGAAGGAGTTGGAGGTGTT, R, CTGGGGTTGGGAGGTAGTTG; GAPDH: F, GTGACGTTGACATCCGTAAAGA, R, GCCGGACTCATCGTACTCC; IL-13: F, CCTCATGGCGCTTTTGTTGAC, R, TCTGGTTCTGGGTGATGTTGA; IL-4: F, CCAACTGCTTCCCCCTCTG, R, TCTGTTACGGTCAACTCGGTG; CXCL1: F, ACCCAAACCGAAGTCATAGC, R, TCTCCGTTACTTGGGGACAC.

Lipid Peroxidation Assay

The lipid hydroperoxide probe Liperfluo (Dojindo, Japan) was used to detect lipid peroxidation in accordance with the manufacturer's protocol. The excitation wavelength was set at 488 nm, and emission was collected within the range of 520–600 nm. The level of ROS in cells was assessed by measuring the oxidative conversion of the cell-permeable compound DCFH-DA to fluorescent dichloro-fluorescein (DCF) using the Reactive Oxygen Species Assay Kit (Nanjing Jiancheng). Imaging was performed using confocal microscopy at a magnification of 100×.

Statistical Analysis

Data are presented as the mean ± standard deviation (SD). A significance level of $p < 0.05$ was determined using a two-tailed Student's *t*-test or one-way analysis of variance (ANOVA).

Results

Data Processing

The procedure of bioinformatics analysis is illustrated in Figure 1. Original datasets for children with AD and control subjects were collected from the GEO dataset GSE107361. The WGCNA and Limma packages in R were utilized to identify key modules and DEGs, and then their intersections were taken to obtain 585 intersections of genes. Subsequently, 1,407 ferroptosis-related genes were obtained from the GeneCards database, and 51 co-expressed genes were identified by intersecting the ferroptosis-related genes with the 585 key AD genes. Three algorithms, LASSO, RF and SVM-RFE, were used to screen these 51 genes to obtain two key genes. At the same time, the 51 genes were analyzed using three Cytoscape algorithms: Maximum Clique Centrality (MCC), Degree, Closeness, and PPI maps were created. Then we searched for 24 target genes of SP in Swiss Target Prediction database and intersected them with ferroptosis-related genes in AD to identifying one associated gene. Experiments were carried out to verify this finding.

Identification of Differentially Expressed Genes (DEGs)

Principal component analysis (PCA) of gene expression in children with AD and in the control group, revealed significant differences between the two groups (Figure 2A). Differential analysis of combined AD and control samples revealed 1,807 DEGs with the cut-off criterion of adjusted $p \leq 0.05$ and $|\log2 \text{ (fold change)}| \geq 1$, containing. Volcano plot and heatmap were utilized to show the expression patterns of DEGs in the integrated AD dataset (Figure 2B and C). The top five enrichment pathways identified by GSEA were the cell cycle, cytokine-cytokine receptor interaction, cytoskeleton in muscle cells, hypertrophic cardiomyopathy, and IL-17 signaling pathway (Figure 2D).

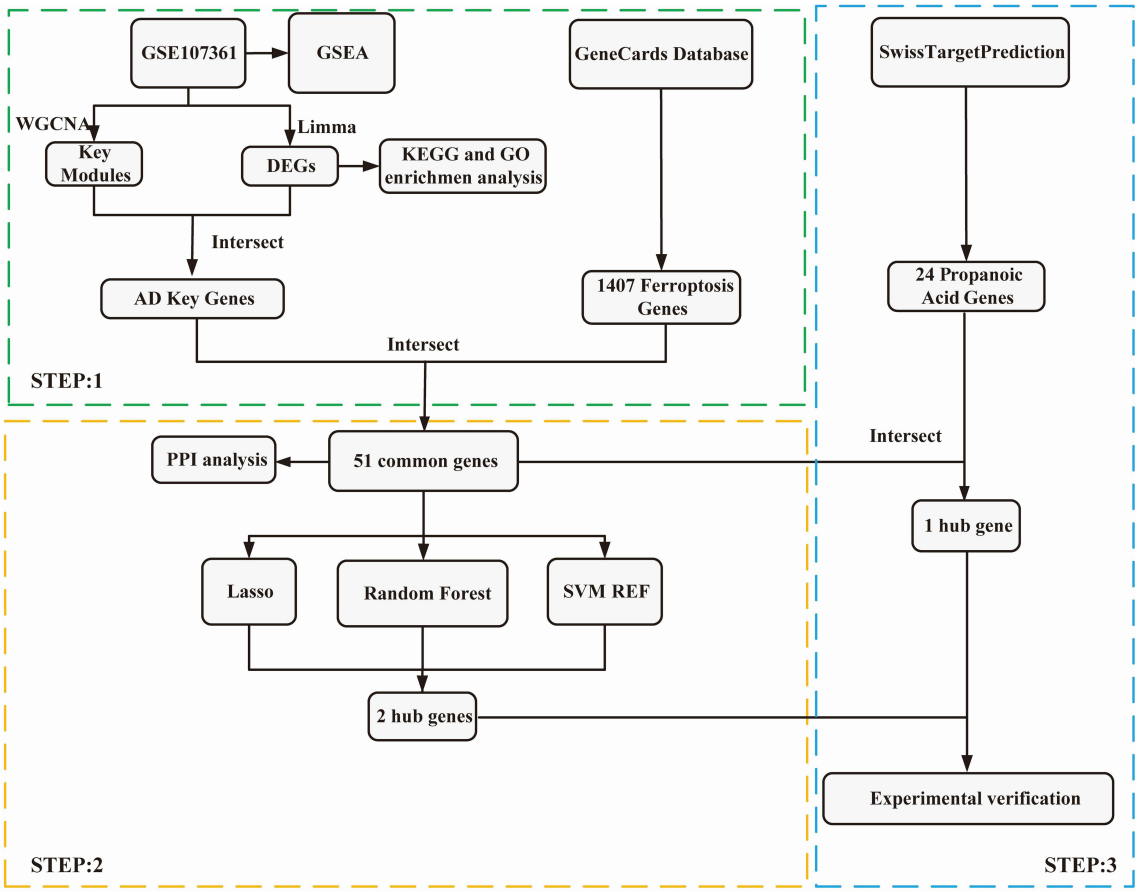

Figure 1 Research design flow chart.

The Construction of Weighted Gene Co-expression Network and the Identification of Key Modules in AD

In order to further investigate the key genes in AD, WGCNA was carried out to identify the most relevant gene modules in skin samples from AD patients. According to the scale independence and average connectivity, the soft-thresholding power of 10 was chosen (Figure 3A and B). Totally seven modules were generated using that power and the cluster dendrogram of the modules was presented in Figure 3C. Furthermore, this study explored the correlation between AD and gene modules (Figure 3D). Finally, blue and turquoise modules with the highest positive correlation and negative correlation were selected. To analyze the biological functions and pathways of these common genes, we performed GO and KEGG analysis. The results of the GO analysis showed that in terms of biological processes (BP), DEGs are mainly associated with the epidermis development, keratinization and skin development. For cellular components (CC), DEGs are mainly associated with collagen-containing extracellular matrix, cornified envelope and secretory granule lumen. In terms of molecular function (MF), DEGs are mainly associated with extracellular matrix structural constituent, glycosaminoglycan binding and peptidase regulator activity. (Figure 3E and Table 1). KEGG pathway analysis showed that DEGs were mainly as sociated with Protein digestion and absorption, cytoskeleton in muscle cells and leukocyte transendothelial migration (Figure 3F). In addition, genes from DEGs were intersected with crucial genes from WGCNA in AD skin samples resulting in 585 genes for further analysis (Figure 3G).

PPI Network Construction and Pathway Analysis

Totally 1,407 genes related to ferroptosis were obtained in Genecards, and 51 key genes were obtained by intersection with the selected key genes of AD (Figure 4A). The key genes for AD were collected by the STRING database with a medium confidence score of >0.4. The pathogenic genes in AD were presented by the Cytoscape software, resulting in

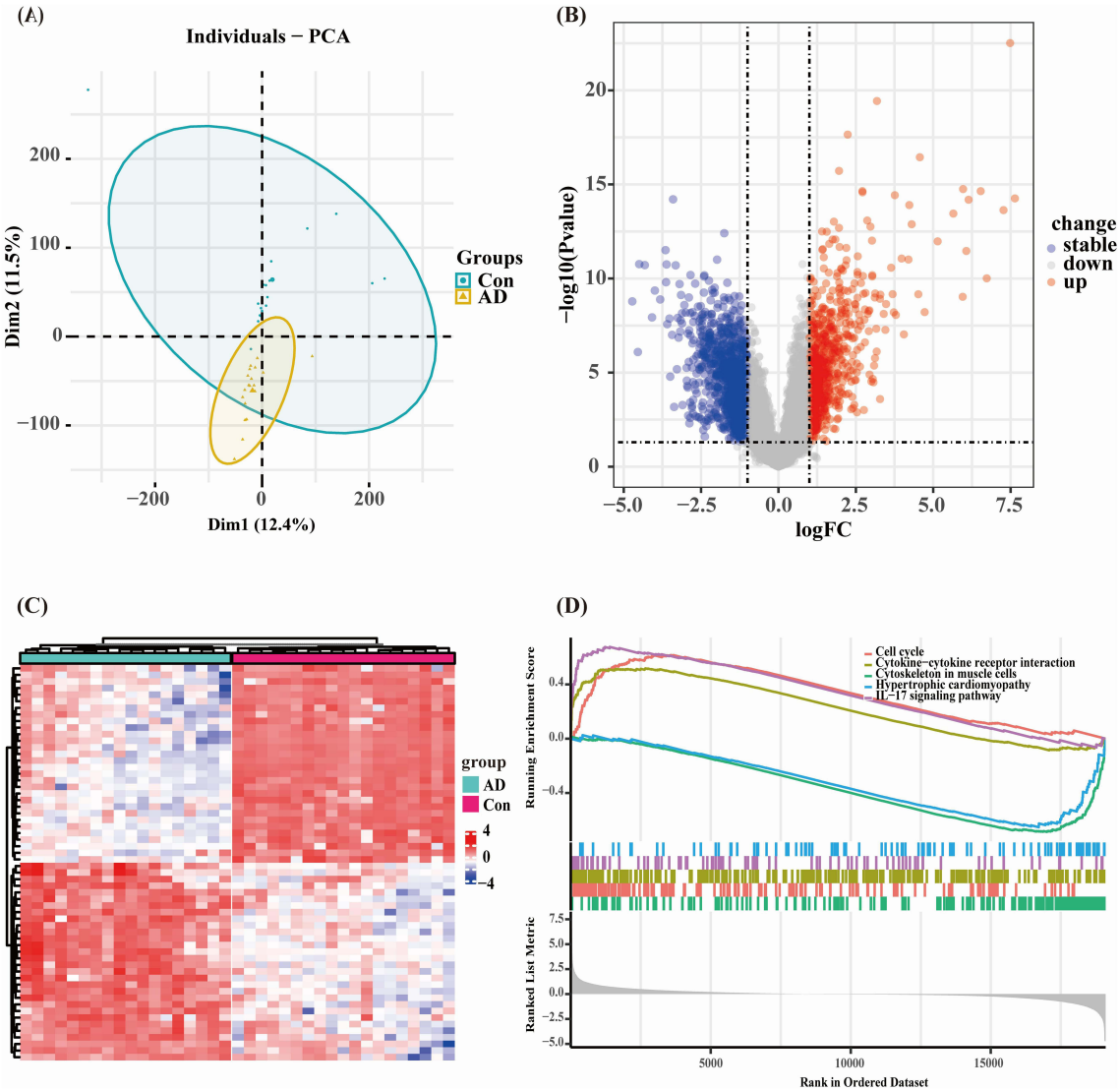

Figure 2 The integration of AD datasets and differential expression analysis of the integrated AD dataset. (**A**) PCA of GSE107361. (**B**) The volcano map of GSE107361. (**C**) Heat map of overlapping CS-DEGs. Upregulated genes are marked in red; downregulated genes are marked in blue. (**D**) GSEA enriches the top five items.

a network contained 51 nodes (Figure 4B and C). These genes were analyzed by GO and KEGG (Figure 4D and E). The results of the GO analysis showed that DEGs are mainly associated with response to metal ion, epidermis development and skin development. KEGG pathway analysis showed that DEGs were mainly as sociated with tight junction, shigellosis and regulation of actin cytoskeleton.

Screening of Hub Genes Harboring Diagnostic Value via Machine Learning and Prediction of Key Genes Associated with SP for Ferroptosis-Related Genes in AD

In this study, we employed three distinct machine learning algorithms—LASSO, RF, and SVM-RFE—to identify key hub genes associated with AD and ferroptosis (Figure 5A–E). The LASSO algorithm pinpointed 8 potential hub genes. The RF algorithm, which ranks genes based on their importance scores, yielded 8 top candidate genes. Similarly, the SVM-RFE algorithm indicated optimum accuracy with a set of 11 genes, leading us to select these as candidates. After crossing the results of the three algorithms, two candidate genes, CDK1 and LTBP2, were obtained (Figure 5F). Next, we intersected 51 ferroptosis-related genes in AD with target genes predicted by SP to obtain the co-expressed gene FABP4 (Figure 5G).

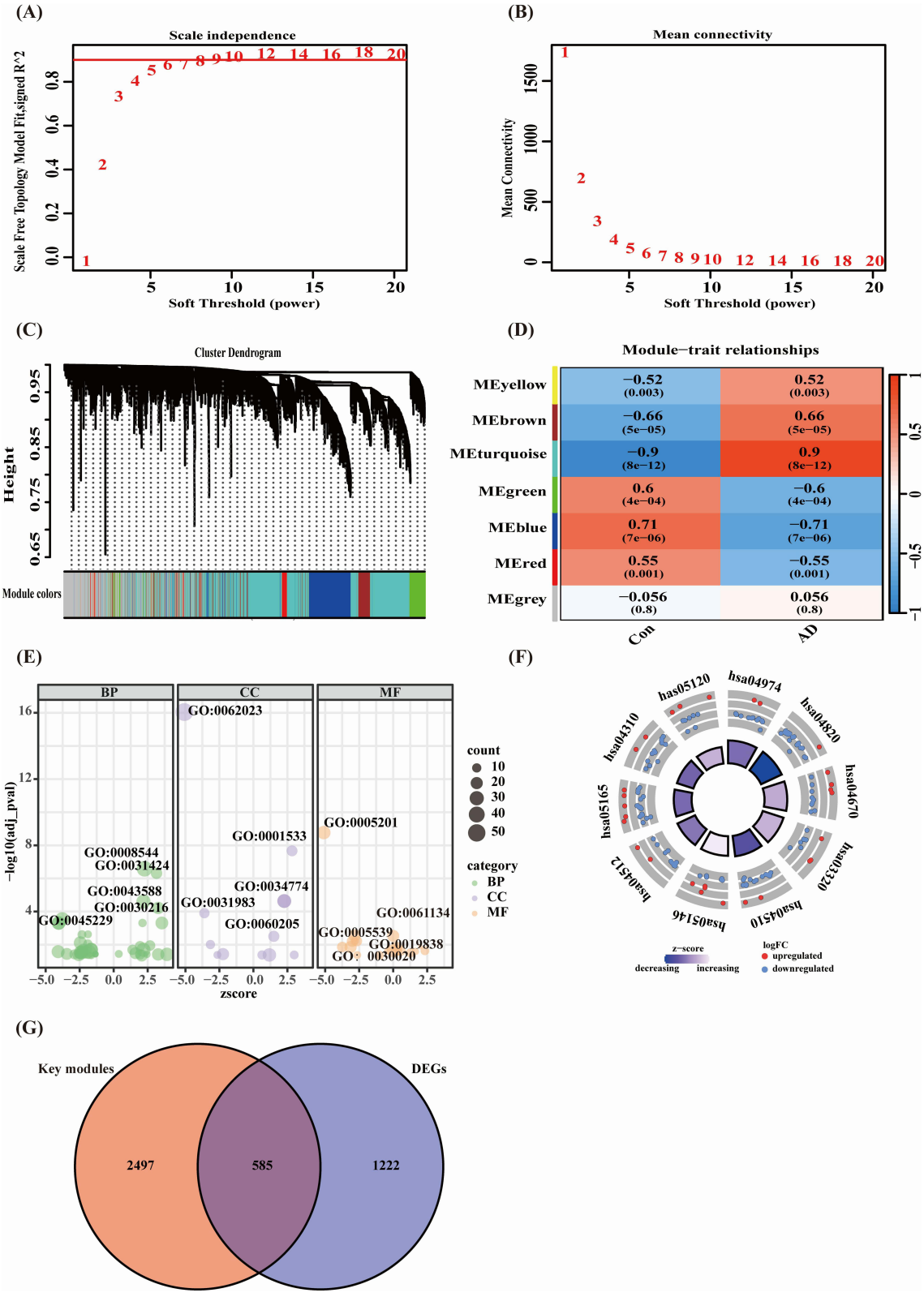

Figure 3 Screening of key module genes in dataset via WGCNA and identification of key genes through the intersection of key module genes and DEGs. (**A** and **B**) The scale-free topology model was utilized to identify the best β value, and β=10 was chosen as the soft threshold based on the average connectivity and scale Independence. (**C**) The network heatmap showing the gene dendrogram and module eigengenes. (**D**) Gene co-expression modules of AD. (**E**) Enrichment results of DEGs GO term. (**F**) Enrichment results of DEGs KEGG pathway. Adjusted p-value<0.05 was significant. (**G**) A total of 585 key genes in AD were identified by taking the intersection between key modules genes and DEGs via the venn diagram.

Table 1 Gene Ontology Analysis of DEGs Associated with AD

Category	Term	Description	Count	*P*
BP	GO:0008544	Epidermis development	38	5.8450668324613E-11
BP	GO:0031424	Keratinization	17	2.184173557314 17E-10
BP	GO:0043588	Skin development	30	1.68112960373939E-08
BP	GO:0030216	Keratinocyte differentiation	21	5.39162789078177E-08
BP	GO:0045229	External encapsulating structure organization	28	3.16526901584993E-07
BP	GO:0009913	Epidermal cell differentiation	23	9.13826601202157E-07
BP	GO:0030198	Extracellular matrix organization	27	9.28208982727832E-07
BP	GO:0018149	Peptide cross-linking	8	9.32127460042889E-07
BP	GO:0043062	Extracellular structure organization	27	9.85974750704488E-07
BP	GO:0072010	Glomerular epithelium development	7	5.29960883534394E-06
CC	GO:0062023	Collagen-containing extracellular matrix	53	1.93280463430554E-19
CC	GO:0001533	Cornified envelope	15	9.29520342334588E-11
CC	GO:0034774	Secretory granule lumen	28	1.9309606241842E-07
CC	GO:0060205	Cytoplasmic vesicle lumen	28	2.33785117065535E-07
CC	GO:0031983	Vesicle lumen	28	2.49026756490138E-07
CC	GO:0005604	Basement membrane	13	1.61277827322962E-06
CC	GO:0005775	Vacuolar lumen	16	0.000047144018571 4118
CC	GO:0005581	Collagen trimer	10	0.000168460706865184
CC	GO:0005788	Endoplasmic reticulum lumen	20	0.000719653773342764
CC	GO:0030175	Filopodium	10	0.00105428827973173
MF	GO:0005201	Extracellular matrix structural constituent	26	2.251450121371 67E-12
MF	GO:0005539	Glycosaminoglycan binding	21	7.46787869032677E-06
MF	GO:0061134	Peptidase regulator activity	20	0.000011821460508065 1
MF	GO:0019838	Growth factor binding	14	0.000038964343562691 4
MF	GO:0030020	Extracellular matrix structural constituent conferring tensile strength	8	0.000040075421690 1847
MF	GO:0008201	Heparin binding	16	0.000049436514317 8136
MF	GO:0050786	RAGE receptor binding	4	0.000128362877813477
MF	GO:0005178	Integrin binding	14	0.000162890477343763
MF	GO:1901681	Sulfur compound binding	20	0.000165567230619364
MF	GO:0030414	Peptidase inhibitor activity	15	0.000185275849218019

SP Inhibits Ferroptosis in HaCaT Cells of AD Models

After the SP intervention, GPX4 and SLC7A11 decreased in the AD cell model, while their expressions increased after intervention (Figure 6A and B). The expression of Ptgs2 and Acsl4 increased in the cell model but decreased after SP intervention (Figure 6C and D). At the same time, ROS and LPO were detected in the cells, and it was found that ROS and LPO expressions increased in the cell model, and decreased after the intervention of SP (Figure 6E). These results indicated that SP improved the ferroptosis phenomenon in the AD cell model.

SP Inhibits the Expression of Inflammatory Genes in HaCaT Cells and Promoted the Expression of Skin Barrier Related Genes

The cell viability rate of HaCaT cells decreased, and cytotoxicity increased under the combined stimulation of TNF-α and IFN-γ, but the cell viability rate increased, and toxicity decreased after the intervention of SP (Figure 7A and B). In cell models, we also validated three key genes that were screened using bioinformatics, LTBP2, FABP4, and CDK1 (Figure 7C and E). IL-4, IL-13, TNF-α, and TSLP were significantly increased in the cell model, and the mRNA expression levels of IL-4, IL-13, TNF-α and TSLP genes were significantly decreased by SP intervention (Figure 7H and J–L). SP treatment significantly enhanced the protein and mRNA expression levels of the FLG and LOR genes encoding skin structural components (Figure 7D, F, G, and I). The expression level of CXCL1 decreased after the intervention of SP, but this trend does not variant (Figure 7M).

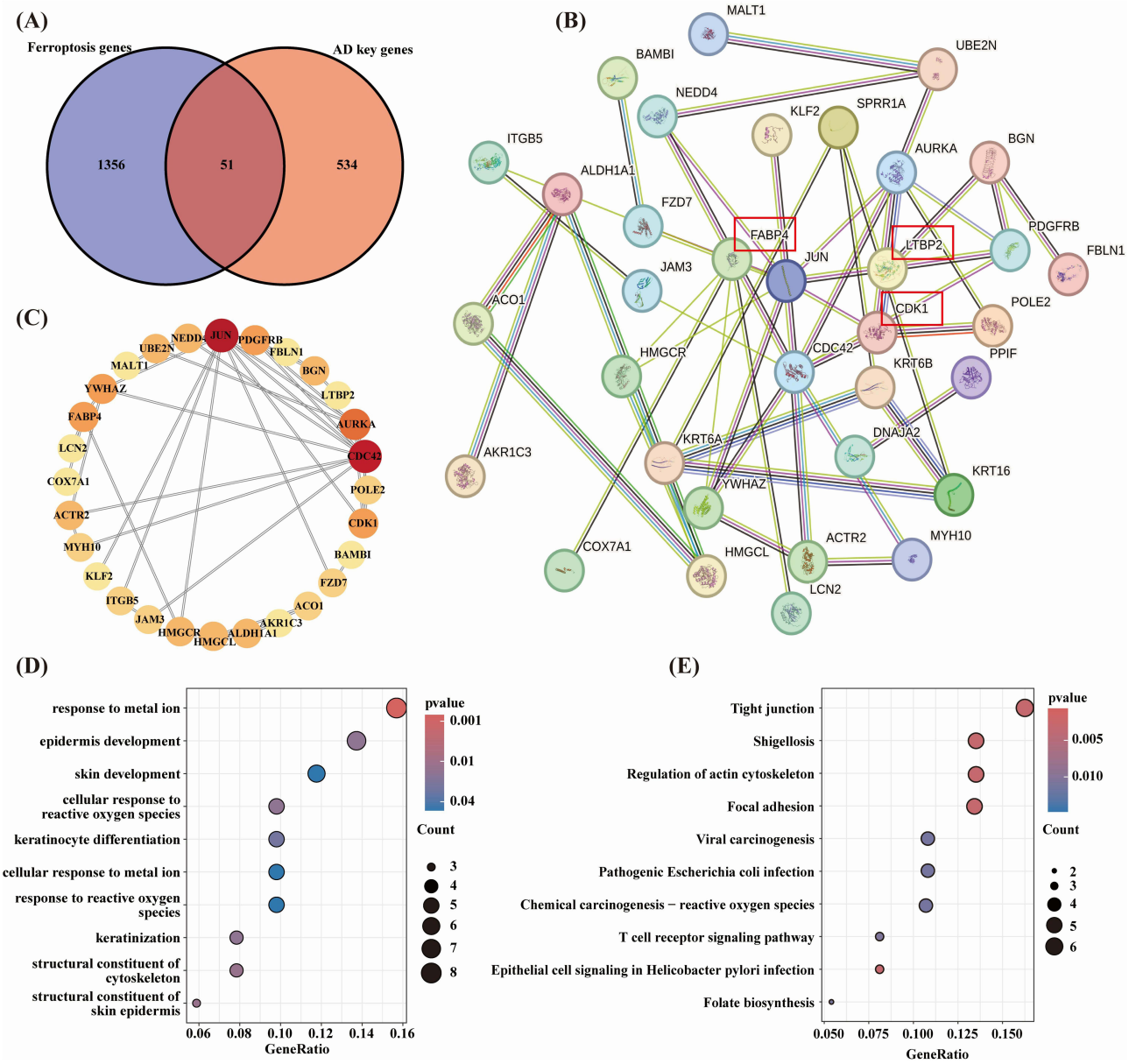

Figure 4 PPI analysis between AD-associated proteins and ferroptosis-related key proteins, and followed by enrichment analysis of the PPI-screened nodes. (**A**) The intersection of AD DEGs with genes coding ferroptosis-related proteins via the venn diagram. (**B** and **C**) PPI network constructed using the STRING database. (**D** and **E**) GO and KEGG maps of key genes.

Discussion

AD is a local, chronic, non-infectious skin disease typically characterized by persistent itching. Repeated attacks of AD bring great burden to families and patients, and greatly reduce the quality of life of patients. At present, there are many treatments for AD, but these methods have more or less negative effects. Even though long-term topical application of corticosteroids is the mainstay of treatment for moderate to severe AD, it can produce some adverse effects.[58] In addition, there has been a reported annual increase in harmful medical conditions following long-term systemic glucocorticoid use in Germany.[59] In addition, immunosuppressive therapy for AD can cause conjunctivitis, and the authors suggest that Janus kinase inhibitors or other therapeutic agents should be considered as soon as possible.[60] In one case report, the patient's AD symptoms did not relieve after the use of immune preparations, but after switching to Baricitinib, both hair loss and AD symptoms were significantly alleviated.[61] Studies have shown that JAK inhibitors, such as abrocitinib, baricitinib, and upadacitinib, are effective options for adolescents with moderate to severe AD, with a rapid onset of

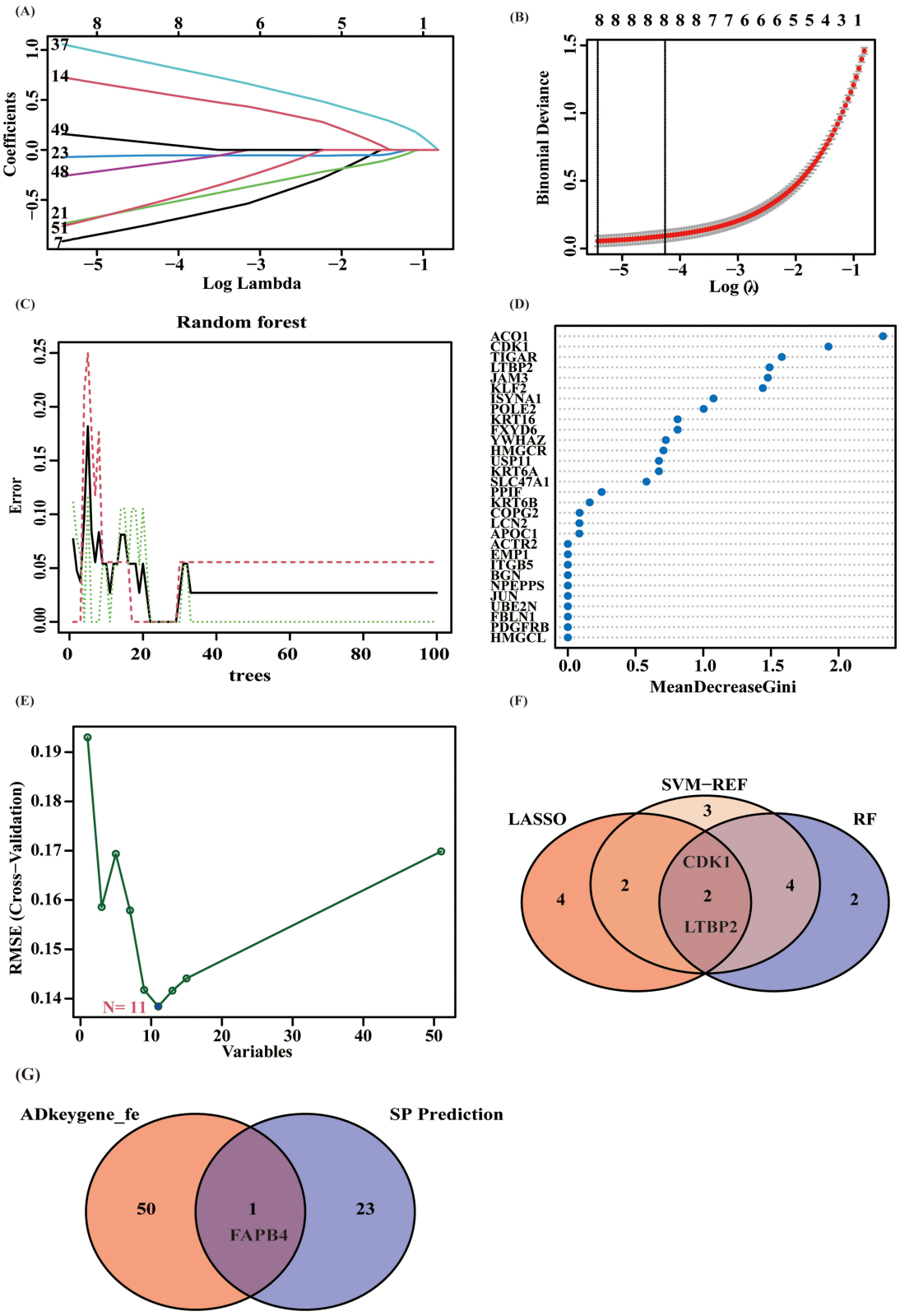

Figure 5 Employing Machine Learning for Identifying Candidate Genes in AD and ferroptosis. (**A** and **B**) Lasso Model for AD Gene Screening. (**C** and **D**) SVM-RFE Model in AD. (**E**) RF Model for AD genes. (**F**) Venn Diagram for AD Candidate Genes. (**G**) Venn Diagram for AD Candidate Genes and predictive SP therapy gene.

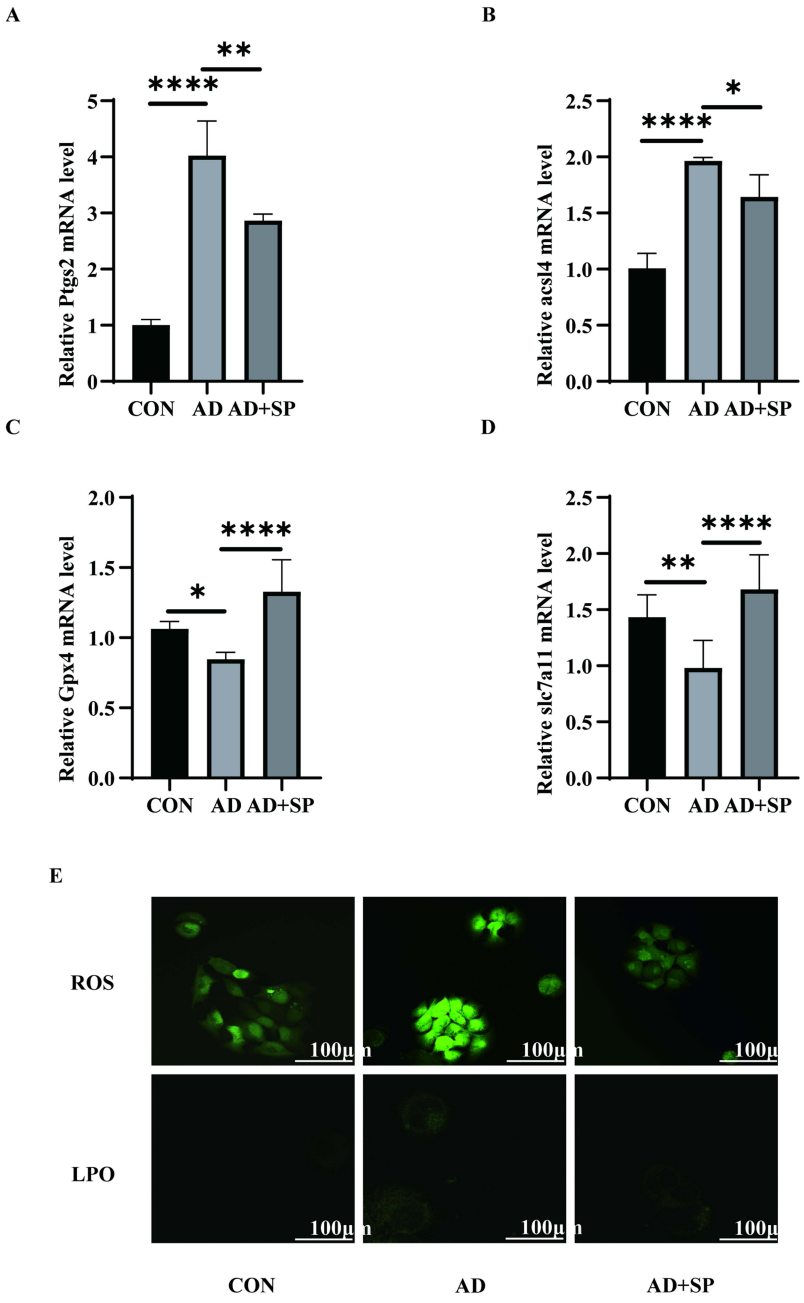

Figure 6 SP improves ferroptosis in AD cell models. (**A**–**D**) mRNA expression of PTGS2, ACSL4, GPX4 and SLC7A11. (**E**) SP improved ROS and LPO levels in AD cell models. *P< 0.05, **P< 0.01, ****P< 0.0001.

action and minimal side effects in subjects.[61] In addition, Japanese researchers have highlighted the good efficacy of JAK inhibitors and have investigated biomarkers for the efficacy of JAK inhibitors on AD, which better reflects the prospect of JAK inhibitors in the application of AD.[29–32] In recent years, there are also some other treatments, which have a better effect on alleviating AD. For example, hydrogel.[62] However, ordinary hydrogels are difficult to quantitatively administer drugs in experiments, so the emergence of Conductive hydrogel can accurately control the dosage.[63] The pathophysiological characteristics of AD are not simple, including genetic, environmental, immune response and other contributing causes. In the United States, the prevalence of AD varies according to diet, and for instance exclusively breastfed infants, mothers supplementing with fruits, vegetables, and prebiotics may have beneficial effects.[64] At the same time, the destruction of microbial balance on the skin surface is an important factor in the pathogenesis of AD.[65] Microorganisms,

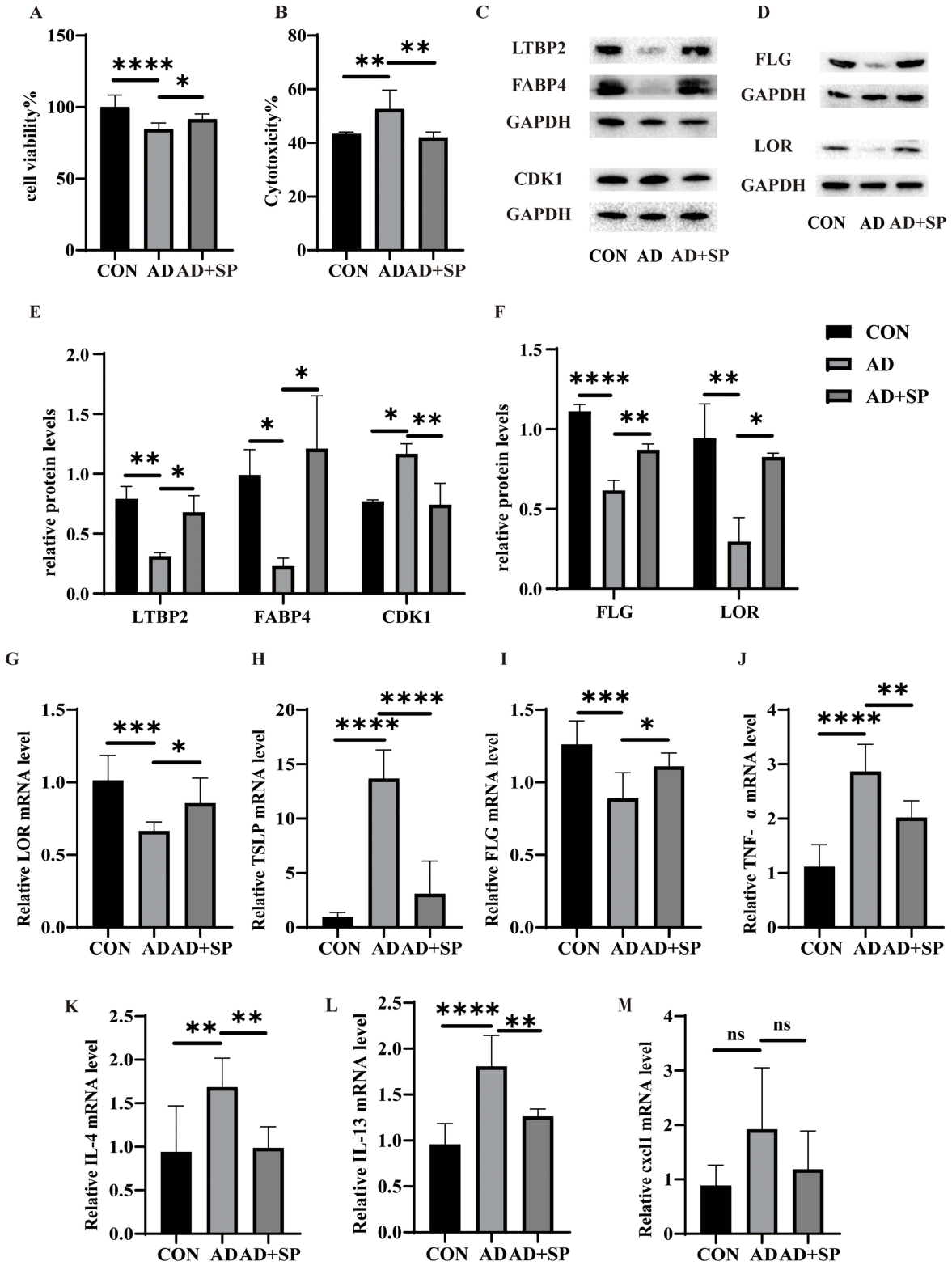

Figure 7 SP improves genes associated with inflammation and skin growth in AD cell models. (**A** and **B**) The cell viability rate and cytotoxicity of AD cell models after SP intervention. (**C**–**F**) Expression of related proteins of LTBP2, FABP4, CDK1, LOR and FLG. (**G**–**M**) mRNA expression of LOR, FLG, TSLP, TNF-α, IL-4,IL-13, and cxcl1. *P< 0.05, **P< 0.01, ***P< 0.001, ****P< 0.0001.

influenced by both environment and diet, play a key role in allergic diseases, and microorganisms can regulate a variety of host cellular processes and immune responses.[66] In this article, we understand the molecular mechanisms of childhood AD that may help in the search for ways to prevent atopic disease. Inflammation is the main characteristic of AD, and inflammation is closely related to oxidative stress, while ferroptosis is closely related to oxidative stress. Meanwhile, SP has been proved effective in improving AD symptoms. So we explored short-chain fatty acids to inhibit ferroptosis and improve AD. We selected dataset GSE107361, searched for key genes, and selected intersection genes with genes related to ferroptosis. In order to better understand the interaction between DEGs, we further performed GO, KEGG pathway and PPI network analysis.

We used R programming language to screen out 585 significantly expressed genes of AD from the data set. Then, 1407 genes related to ferroptosis were obtained from Genecards, and 51 genes co-expressed by AD and ferroptosis were obtained by intersection of these 585 and 1407 genes, and the pathways and functions of these key genes were explored. The results of the GO analysis showed that DEGs are mainly associated with response to metal ion, epidermis development, and skin development. KEGG pathway analysis showed that DEGs were mainly as sociated with tight junction, shigellosis and regulation of actin cytoskeleton. Therefore, all of these pathways may be involved in the pathogenesis of childhood AD. At the same time, the analysis based on PPI network shows that JUN, CDC42, AURKA, FABP4, and CDK1 exhibit the highest number of intermediaries and belong to the key modules of PPI network. We then used three machine learning algorithms to obtain two key genes, CDK1 and LTBP2. Machine learning plays an important role in solving clinical problems.[67] Finally, the therapeutic targets of SP were obtained from the drug target prediction website, and the intersection of these target genes with 51 genes screened to obtain FABP4, which is the key therapeutic target of SP on AD.

In a study that analyzed four GSE datasets, the key genes identified for AD included CDK1 and PTGS2.[27] This finding is verified by the results of the screening conducted in this study. CDK1 is a cyclin-dependent kinase 1 that is highly expressed in skin cancer,[68] Skin cancer tissue has 33 times more CDK1 than in normal skin.[69] It is also highly expressed in melanoma.[70] Knockdown of CDK1 in cells experiments can inhibit the development of melanoma.[71] Inhibition of CDK1 in cells can block cell proliferation, migration, and invasion in psoriasis.[72] PTGS2 is a gene in human skin that is sensitive to ultraviolet light,[73] PTGS2 is a key gene in ferroptosis and a potential regulator of targeted immunity and inflammation. In a passive cutaneous anaphylaxis mouse model, inhibit PTGS2 can significantly inhibit mast cell degranulation and reduce inflammatory cytokines, increase vascular barrier.[74] Studies have shown that PTGS2 is involved in skin inflammation and apoptosis caused by ultraviolet light, and topical inhibitors of PTGS2 can effectively improve photosensitive skin keratosis.[73] However, the mechanism of PTGS2 inhibitors in skin malignant diseases is complex and not fully understood. In this study, we explored that SP reduces the expression of PTGS2 in AD model of HaCaT cells by blocking ferroptosis, which not only lays the foundation for SP to improve skin diseases, but also helps to reduce the expression of PTGS2 in AD model of HaCaT cells. It also provides in vitro experimental basis for evaluating the local use of non-steroidal anti-inflammatory drugs to prevent high-risk skin diseases. One study shown that in the small extracellular vesicles of HIV patients, the expression of LTBP2 is down-regulated in human adipocytes with dystrophia, and the down-regulation of LTBP2 causes the down-regulation of FABP4.[75] LTBP2 is a potential TGF-β-binding protein 2,[76] It is a multi-domain extracellular matrix protein localized to chromosome 14q24.3.[77] Studies have shown that LTBP2 can act as a binding protein for EGF-likeprotein, which is critical for the formation of elastic fibers that play a major role in providing elasticity and integrity in skin tissue.[78] In addition, LTBP2 may act as a molecular switch to determine the location of EGF-likeprotein deposition, thereby regulating the subfiber assembly of elastic fiber components.[78] Downregulation of LTBP2 may cause dysregulation of adipose differentiation and inflammatory responses, which may cause associated metabolic disorders and inflammatory fluctuations.[75]

FABP4 is a recently discovered fatty acid-binding protein that can work with adenosine kinase to form a functional hormone complex that regulates ATP levels inside and outside cells.[79] In addition, the lack of FABP4/FABP5 in T cells can cause the uptake efficiency of exogenous free fatty acids by $CD8^{+}T_{RM}$cells. In addition, skin $CD8^{+}T_{RM}$cells knocked out by FABP4/FABP5 showed poor protection against skin virus infection in mice.[80] Patrick M Brunner et al examined blood samples from 30 AD patients under 5 years of age by high throughput and found that FABP4 expression was

decreased relative to the normal group.[81] Another study that included four datasets, also showed decreased expression of ferroptosis-related gene FABP4 in AD samples.[26] These are consistent with the results of this paper.

In summary, we identified genes that differ in the expression of genes associated with ferroptosis in childhood AD, while looking for therapeutic targets for SP, and explored the potential functions and related pathways involved in the pathogenesis of childhood AD. In addition, our study shows that LTBP2 and FABP4 play a crucial role in the molecular mechanism of childhood AD.

However, there are still some shortcomings in this study. Only one GSE dataset was obtained, which may lead to bias in results. Secondly, the therapeutic effect of SP on AD was only explored in cell experiments, without experimental verification in animal experiments. At the same time, no key pathway genes were knocked out or overexpressed to further explore the up-regulation effect of SP on LTBP2 and FABP4, and the improvement effect of up-regulation of LTBP2 by SP on AD. In future studies, if conditions permit, we will collect more blood or skin samples from children with AD, reduce the deviation of results, and explore and verify them in animal experiments. In particular, further research is needed to validate CDK1, LTBP2, and FABP4, which can be considered key genes involved in childhood AD with potential for diagnostic and therapeutic applications.

Conclusion

We performed bioinformatics analysis on the GEO dataset to explore the underlying molecular mechanisms and key genes for the development of ferroptosis of AD. Through three machine learning algorithms, LASSO, RF, and SVM-RFE, we identified three genes, CDK1, LTBP2 and FABP4, as potential therapeutic targets and biomarkers of SP for the development of ferroptosis of AD. Based on these 3 genes, we have generated a new understanding of the pathogenesis of ferroptosis in AD and may be an interesting target for future in-depth studies.

Funding

This work was supported by the Jiangsu Provincial Department of Science and Technology (No. BE2022698), the Postgraduate Research & Practice Innovation Program of Jiangsu Province (No.KYCX23_2572 to Dr. Xie), and the Wuxi Municipal Science and Technology Bureau (No.Y20222003).

Disclosure

The author(s) report no conflicts of interest in this work.

References

1. Silverberg JI, Barbarot S, Gadkari A, et al. Atopic dermatitis in the pediatric population: a cross-sectional, international epidemiologic study. *Ann Allergy Asthma Immunol*. 2021;126(4):417–428.e2. doi:10.1016/j.anai.2020.12.020
2. Lavazais S, Jargosch M, Dupont S, et al. IRAK4 inhibition dampens pathogenic processes driving inflammatory skin diseases. *Sci Transl Med*. 2023;15(683):eabj3289. doi:10.1126/scitranslmed.abj3289
3. Guttman-Yassky E, Lowes MA, Fuentes-Duculan J, et al. Low expression of the IL-23/Th17 pathway in atopic dermatitis compared to psoriasis. *J Immunol*. 2008;181(10):7420–7427. doi:10.4049/jimmunol.181.10.7420
4. Li L, Mu Z, Liu P, et al. Mdivi-1 alleviates atopic dermatitis through the inhibition of NLRP3 inflammasome. *Exp Dermatol*. 2021;30 (12):1734–1744. doi:10.1111/exd.14412
5. Yao Y, Wang Z, Li J, et al. Pyroptosis and its role in autoimmune skin disease. *Exp Dermatol*. 2024;33(7):e15135. doi:10.1111/exd.15135
6. Gallegos-Alcalá P, Jiménez M, Cervantes-García D, et al. Glycomacropeptide protects against inflammation and oxidative stress, and promotes wound healing in an atopic dermatitis model of human keratinocytes. *Foods*. 2023;12(10):1932. doi:10.3390/foods12101932
7. Gupta RK, Miller J, Croft M. TNF-like weak inducer of apoptosis inhibition is comparable to IL-13 blockade in ameliorating atopic dermatitis inflammation. *Allergy*. 2024;79(1):116–127. doi:10.1111/all.15879
8. Ye B, Hu W, Yu G, et al. A cascade-amplified pyroptosis inducer: optimizing oxidative stress microenvironment by self-supplying reactive nitrogen species enables potent cancer immunotherapy. *ACS Nano*. 2024;18(26):16967–16981. doi:10.1021/acsnano.4c03172
9. Askari H, Rajani SF, Poorebrahim M, et al. A glance at the therapeutic potential of irisin against diseases involving inflammation, oxidative stress, and apoptosis: an introductory review. *Pharmacol Res*. 2018;129:44–55. doi:10.1016/j.phrs.2018.01.012
10. Bell HN, Stockwell BR, Zou W. Ironing out the role of ferroptosis in immunity. *Immunity*. 2024;57(5):941–956. doi:10.1016/j.immuni.2024.03.019
11. Zhang D, Li Y, Du C, et al. Evidence of pyroptosis and ferroptosis extensively involved in autoimmune diseases at the single-cell transcriptome level. *J Transl Med*. 2022;20(1):363. doi:10.1186/s12967-022-03566-6
12. Yu Y, Yan Y, Niu F, et al. Ferroptosis: a cell death connecting oxidative stress, inflammation and cardiovascular diseases. *Cell Death Discov*. 2021;7 (1):193. doi:10.1038/s41420-021-00579-w

13. Yan N, Xu Z, Qu C, et al. Dimethyl fumarate improves cognitive deficits in chronic cerebral hypoperfusion rats by alleviating inflammation, oxidative stress, and ferroptosis via NRF2/ARE/NF-κB signal pathway. *Int Immunopharmacol*. 2021;98:107844. doi:10.1016/j.intimp.2021.107844
14. Zuo X, Zeng H, Wang B, et al. AKR1C1 protects corneal epithelial cells against oxidative stress-mediated ferroptosis in dry eye. *Invest Ophthalmol Vis Sci*. 2022;63(10):3. doi:10.1167/iovs.63.10.3
15. Wang Y, Liao S, Pan Z, et al. Hydrogen sulfide alleviates particulate matter-induced emphysema and airway inflammation by suppressing ferroptosis. *Free Radic Biol Med*. 2022;186:1–16. doi:10.1016/j.freeradbiomed.2022.04.014
16. Sun Y, Chen P, Zhai B, et al. The emerging role of ferroptosis in inflammation. *Biomed Pharmacother*. 2020;127:110108. doi:10.1016/j.biopha.2020.110108
17. Deng L, He S, Guo N, et al. Molecular mechanisms of ferroptosis and relevance to inflammation. *Inflamm Res*. 2023;72(2):281–299. doi:10.1007/s00011-022-01672-1
18. Shou Y, Yang L, Yang Y, et al. Inhibition of keratinocyte ferroptosis suppresses psoriatic inflammation. *Cell Death Dis*. 2021;12(11):1009. doi:10.1038/s41419-021-04284-5
19. Vats K, Kruglov O, Mizes A, et al. Keratinocyte death by ferroptosis initiates skin inflammation after UVB exposure. *Redox Biol*. 2021;47:102143. doi:10.1016/j.redox.2021.102143
20. Gong Z, Wang Y, Li L, et al. Cardamonin alleviates chondrocytes inflammation and cartilage degradation of osteoarthritis by inhibiting ferroptosis via p53 pathway. *Food Chem Toxicol*. 2023;174:113644. doi:10.1016/j.fct.2023.113644
21. Jia Y, Hu J, An K, et al. Hydrogel dressing integrating FAK inhibition and ROS scavenging for mechano-chemical treatment of atopic dermatitis. *Nat Commun*. 2023;14(1):2478. doi:10.1038/s41467-023-38209-x
22. He T, Tang W, Chen J, et al. Hydrogel-based treatment of house dust mite-induced atopic dermatitis through triple cleaning of mites, bacteria, and ROS-related inflammation. *ACS Appl Mater Interfaces*. 2024;16(26):33121–33134. doi:10.1021/acsami.4c05435
23. Trinh TA, Nguyen TL, Kim J. Lignin-based antioxidant hydrogel patch for the management of atopic dermatitis by mitigating oxidative stress in the skin. *ACS Appl Mater Interfaces*. 2024;16(26):33135–33148. doi:10.1021/acsami.4c05523
24. Wu KL, Chan SH, Chan JY. Neuroinflammation and oxidative stress in rostral ventrolateral medulla contribute to neurogenic hypertension induced by systemic inflammation. *J Neuroinflammation*. 2012;9:212. doi:10.1186/1742-2094-9-212
25. Sun S, Shen J, Jiang J, et al. Targeting ferroptosis opens new avenues for the development of novel therapeutics. *Signal Transduct Target Ther*. 2023;8(1):372. doi:10.1038/s41392-023-01606-1
26. Xu L, Guo W, Hao H, et al. Computational recognition of regulator genes and signature for ferroptosis with implications on immunological properties and clinical management of atopic dermatitis. *Front Immunol*. 2024;15:1412382. doi:10.3389/fimmu.2024.1412382
27. Wang T, Zhang B, Li D, Qi X, Zhang C. Bioinformatic analysis of key pathways and genes involved in pediatric atopic dermatitis. *Biosci Rep*. 2021;41(1):BSR20193517.
28. Chu DK, Chu DK, Schneider L, et al. Atopic dermatitis (eczema) guidelines: 2023 American Academy of Allergy, Asthma and Immunology/American College of Allergy, Asthma and Immunology Joint Task Force on Practice Parameters GRADE- and institute of medicine-based recommendations. *Ann Allergy Asthma Immunol*. 2024;132(3):274–312. doi:10.1016/j.anai.2023.11.009
29. Hagino T, Saeki H, Fujimoto E, et al. Efficacy and safety of baricitinib treatment for moderate to severe atopic dermatitis in real-world practice in Japan. *J Dermatol*. 2023;50(7):869–879. doi:10.1111/1346-8138.16763
30. Hagino T, Hamada R, Yoshida M, et al. Total eosinophil count as a biomarker for therapeutic effects of upadacitinib in atopic dermatitis over 48 weeks. *Front Immunol*. 2024;15:1365544. doi:10.3389/fimmu.2024.1365544
31. Hagino T, Saeki H, Kanda N. The efficacy and safety of upadacitinib treatment for moderate to severe atopic dermatitis in real-world practice in Japan. *J Dermatol*. 2022;49(11):1158–1167. doi:10.1111/1346-8138.16549
32. Hagino T, Yoshida M, Hamada R, et al. Predictive factors for responders to upadacitinib treatment in patients with atopic dermatitis. *J DermatolTreat*. 2024;35(1):2310643. doi:10.1080/09546634.2024.2310643
33. Thomsen M, Künstner A, Wohlers I, et al. A comprehensive analysis of gut and skin microbiota in canine atopic dermatitis in Shiba Inu dogs. *Microbiome*. 2023;11(1):232. doi:10.1186/s40168-023-01671-2
34. Voigt J, Lele M. Lactobacillus rhamnosus used in the perinatal period for the prevention of atopic dermatitis in infants: a systematic review and meta-analysis of randomized trials. *Am J Clin Dermatol*. 2022;23(6):801–811. doi:10.1007/s40257-022-00723-x
35. Wang IJ, Wang JY. Children with atopic dermatitis show clinical improvement after Lactobacillus exposure. *Clin Exp Allergy*. 2015;45(4):779–787. doi:10.1111/cea.12489
36. Zheng DW, Li R-Q, An J-X, et al. Prebiotics-encapsulated probiotic spores regulate gut microbiota and suppress colon cancer. *Adv Mater*. 2020;32(45):e2004529. doi:10.1002/adma.202004529
37. Liu H, Cai Z, Wang F, et al. Colon-targeted adhesive hydrogel microsphere for regulation of gut immunity and flora. *Adv Sci*. 2021;8(18):e2101619. doi:10.1002/advs.202101619
38. Filippone A, Lanza M, Campolo M, et al. The anti-inflammatory and antioxidant effects of sodium propionate. *Int J Mol Sci*. 2020;21(8):3026. doi:10.3390/ijms21083026
39. Tong LC, Wang Y, Wang Z-B, et al. Propionate ameliorates dextran sodium sulfate-induced colitis by improving intestinal barrier function and reducing inflammation and oxidative stress. *Front Pharmacol*. 2016;7:253. doi:10.3389/fphar.2016.00253
40. Wang J, Wei Z, Zhang X, et al. Propionate protects against lipopolysaccharide-induced mastitis in mice by restoring blood-milk barrier disruption and suppressing inflammatory response. *Front Immunol*. 2017;8:1108. doi:10.3389/fimmu.2017.01108
41. Liu L, Wu W, Li J, et al. Two sesquiterpene aminoquinones protect against oxidative injury in HaCaT keratinocytes via activation of AMPKα/ERK-Nrf2/ARE/HO-1 signaling. *Biomed Pharmacother*. 2018;100:417–425. doi:10.1016/j.biopha.2018.02.034
42. Xiao Q, Guo J, Lu Y, et al. Molybdenum nanoparticles alleviate MC903-induced atopic dermatitis-like symptoms in mice by modulating the ROS-mediated NF-κB and Nrf2 /HO-1 signaling pathways. *Int J Nanomed*. 2024;19:8779–8796. doi:10.2147/IJN.S472999
43. Chen D, Gao Z-Q, Wang -Y-Y, et al. Sodium propionate enhances Nrf2-mediated protective defense against oxidative stress and inflammation in lipopolysaccharide-induced neonatal mice. *J Inflamm Res*. 2021;14:803–816. doi:10.2147/JIR.S303105
44. Chen X, Su W, Wan T, et al. Sodium butyrate regulates Th17/Treg cell balance to ameliorate uveitis via the Nrf2/HO-1 pathway. *Biochem Pharmacol*. 2017;142:111–119. doi:10.1016/j.bcp.2017.06.136

45. Tang Y, Chen Y, Jiang H, et al. The role of short-chain fatty acids in orchestrating two types of programmed cell death in colon cancer. *Autophagy*. 2011;7(2):235–237. doi:10.4161/auto.7.2.14277
46. Wu YL, Zhang C-H, Teng Y, et al. Propionate and butyrate attenuate macrophage pyroptosis and osteoclastogenesis induced by CoCrMo alloy particles. *Mil Med Res*. 2022;9(1):46. doi:10.1186/s40779-022-00404-0
47. Qiu Z, Zhu Z, Liu X, et al. A dysregulated sebum-microbial metabolite-IL-33 axis initiates skin inflammation in atopic dermatitis. *J Exp Med*. 2022;219(10). doi:10.1084/jem.20212397
48. Xu Y, Qiu Z, Gu C, et al. Propionate alleviates itch in murine models of atopic dermatitis by modulating sensory TRP channels of dorsal root ganglion. *Allergy*. 2024;79(5):1271–1290. doi:10.1111/all.15998
49. Barrett T, Wilhite SE, Ledoux P, et al. NCBI GEO: archive for functional genomics data sets--update. *Nucleic Acids Res*. 2013;41(Database issue): D991–5. doi:10.1093/nar/gks1193
50. Daina A, Michielin O, Zoete V. SwissTargetPrediction: updated data and new features for efficient prediction of protein targets of small molecules. *Nucleic Acids Res*. 2019;47(W1):W357–w364. doi:10.1093/nar/gkz382
51. Subramanian A, Tamayo P, Mootha VK, et al. Gene set enrichment analysis: a knowledge-based approach for interpreting genome-wide expression profiles. *Proc Natl Acad Sci USA*. 2005;102(43):15545–15550. doi:10.1073/pnas.0506580102
52. Yu G, Wang L-G, Han Y, et al. clusterProfiler: an R package for comparing biological themes among gene clusters. *Omics*. 2012;16(5):284–287. doi:10.1089/omi.2011.0118
53. Friedman J, Hastie T, Tibshirani R. Regularization paths for generalized linear models via coordinate descent. *J Stat Softw*. 2010;33(1):1–22. doi:10.18637/jss.v033.i01
54. Huang S, Cai N, Pacheco PP, et al. Applications of Support Vector Machine (SVM) learning in cancer genomics. *Cancer Genomics Proteomics*. 2018;15(1):41–51. doi:10.21873/cgp.20063
55. Petralia F, Wang P, Yang J, et al. Integrative random forest for gene regulatory network inference. *Bioinformatics*. 2015;31(12):i197–205. doi:10.1093/bioinformatics/btv268
56. Szklarczyk D, Gable AL, Lyon D, et al. STRING v11: protein-protein association networks with increased coverage, supporting functional discovery in genome-wide experimental datasets. *Nucleic Acids Res*. 2019;47(D1):D607–d613. doi:10.1093/nar/gky1131
57. Smoot ME, Ono K, Ruscheinski J, et al. Cytoscape 2.8: new features for data integration and network visualization. *Bioinformatics*. 2011;27 (3):431–432. doi:10.1093/bioinformatics/btq675
58. Jang YH, Choi E-Y, Lee H, et al. Long-term use of oral corticosteroids and safety outcomes for patients with atopic dermatitis. *JAMA Network Open*. 2024;7(7):e2423563. doi:10.1001/jamanetworkopen.2024.23563
59. Hagenström K, Klinger T, Müller K, et al. Utilization and related harms of systemic glucocorticosteroids for atopic dermatitis: claims data analysis. *Br J Dermatol*. 2024;191(5):719–727. doi:10.1093/bjd/ljae250
60. Reguiai Z, Becherel PA, Perrot JL, et al. Evolution of dupilumab-associated conjunctivitis in patients with atopic dermatitis after switching dupilumab to tralokinumab or Janus kinase inhibitors (RESO - ADOC study). *J Eur Acad Dermatol Venereol*. 2024;38(11):2149–2155. doi:10.1111/jdv.20233
61. Fang H, Zhang F, Lin W, et al. Case report: sequential therapy with dupilumab and baricitinib for severe alopecia areata with atopic dermatitis in children. *Front Immunol*. 2024;15:1395288. doi:10.3389/fimmu.2024.1395288
62. Cao H, Wang M, Ding J, et al. Hydrogels: a promising therapeutic platform for inflammatory skin diseases treatment. *J Mater Chem B*. 2024;12 (33):8007–8032. doi:10.1039/D4TB00887A
63. Liang Q, Xiang H, Xin M, et al. A wearable iontophoresis enables dual-responsive transdermal delivery for atopic dermatitis treatment. *J Colloid Interface Sci*. 2025;678(Pt A):908–919. doi:10.1016/j.jcis.2024.08.209
64. Khan A, Adalsteinsson J, Whitaker-Worth DL. Atopic dermatitis and nutrition. *Clin Dermatol*. 2022;40(2):135–144. doi:10.1016/j.clindermatol.2021.10.006
65. Koh LF, Ong RY, Common JE. Skin microbiome of atopic dermatitis. *Allergol Int*. 2022;71(1):31–39. doi:10.1016/j.alit.2021.11.001
66. Losol P, Wolska M, Wypych TP, et al. A cross talk between microbial metabolites and host immunity: its relevance for allergic diseases. *Clin Transl Allergy*. 2024;14(2):e12339. doi:10.1002/clt2.12339
67. Deo RC. Machine learning in medicine. *Circulation*. 2015;132(20):1920–1930. doi:10.1161/CIRCULATIONAHA.115.001593
68. Lee PS, Chiou Y-S, Chou P-Y, et al. 3'-Hydroxypterostilbene Inhibits 7,12-Dimethylbenz[a]anthracene (DMBA)/12-O-Tetradecanoylphorbol-13-Acetate (TPA)-induced mouse skin carcinogenesis. *Phytomedicine*. 2021;81:153432. doi:10.1016/j.phymed.2020.153432
69. Balasubramanian S, Ahmad N, Jeedigunta S, et al. Alterations in cell cycle regulation in mouse skin tumors. *Biochem Biophys Res Commun*. 1998;243(3):744–748. doi:10.1006/bbrc.1998.8172
70. Luan H, Jian L, He Y, et al. Exploration and validation of metastasis-associated genes for skin cutaneous melanoma. *Sci Rep*. 2022;12(1):13002. doi:10.1038/s41598-022-17468-6
71. Sun W, Zhao F, Xu Y, et al. Chondroitin polymerizing factor (CHPF) promotes development of malignant melanoma through regulation of CDK1. *Cell Death Dis*. 2020;11(7):496. doi:10.1038/s41419-020-2526-9
72. Fang Y, E C, Wu S, et al. Circ-IGF1R plays a significant role in psoriasis via regulation of a miR-194-5p/CDK1 axis. *Cytotechnology*. 2021;73 (6):775–785. doi:10.1007/s10616-021-00496-x
73. Zhan H, Zheng H. The role of topical cyclo-oxygenase-2 inhibitors in skin cancer: treatment and prevention. *Am J Clin Dermatol*. 2007;8 (4):195–200. doi:10.2165/00128071-200708040-00002
74. Chen Y, Jian X, Zhu L, et al. PTGS2: a potential immune regulator and therapeutic target for chronic spontaneous urticaria. *Life Sci*. 2024;344:122582. doi:10.1016/j.lfs.2024.122582
75. Srinivasa S, Garcia-Martin R, Torriani M, et al. Altered pattern of circulating miRNAs in HIV lipodystrophy perturbs key adipose differentiation and inflammation pathways. *JCI Insight*. 2021;6(18). doi:10.1172/jci.insight.150399
76. Wu J, Subbaiah KCV, Xie LH, et al. Glutamyl-Prolyl-tRNA synthetase regulates proline-rich pro-fibrotic protein synthesis during cardiac fibrosis. *Circ Res*. 2020;127(6):827–846. doi:10.1161/CIRCRESAHA.119.315999
77. Ali M, McKibbin M, Booth A, et al. Null mutations in LTBP2 cause primary congenital glaucoma. *Am J Hum Genet*. 2009;84(5):664–671. doi:10.1016/j.ajhg.2009.03.017

78. Hirai M, Horiguchi M, Ohbayashi T, et al. Latent TGF-beta-binding protein 2 binds to DANCE/fibulin-5 and regulates elastic fiber assembly. *EMBO j*. 2007;26(14):3283–3295. doi:10.1038/sj.emboj.7601768
79. Prentice KJ, Saksi J, Robertson LT, et al. A hormone complex of FABP4 and nucleoside kinases regulates islet function. *Nature*. 2021;600 (7890):720–726. doi:10.1038/s41586-021-04137-3
80. Pan Y, Tian T, Park CO, et al. Survival of tissue-resident memory T cells requires exogenous lipid uptake and metabolism. *Nature*. 2017;543 (7644):252–256. doi:10.1038/nature21379
81. Brunner PM, He H, Pavel AB, et al. The blood proteomic signature of early-onset pediatric atopic dermatitis shows systemic inflammation and is distinct from adult long-standing disease. *J Am Acad Dermatol*. 2019;81(2):510–519. doi:10.1016/j.jaad.2019.04.036